Cardiovascular Research (2016) **112**, 555–567
doi:10.1093/cvr/cvw204

The nuclear pore protein Nup153 associates with chromatin and regulates cardiac gene expression in dystrophic *mdx* hearts

Simona Nanni[1], Agnese Re[2], Cristian Ripoli[3], Aoife Gowran[4], Patrizia Nigro[4], Domenico D'Amario[5], Antonio Amodeo[6], Filippo Crea[5], Claudio Grassi[3,7], Alfredo Pontecorvi[1], Antonella Farsetti[2,8]*, and Claudia Colussi[2]*

[1]Institute of Medical Pathology, Università Cattolica, Rome 00168, Italy; [2]Institute of Cell Biology and Neurobiology, National Research Council, Rome 00143, Italy; [3]Institute of Human Physiology, Medical School, Università Cattolica, Rome 00168, Italy; [4]Unit of Vascular Biology and Regenerative Medicine, Centro Cardiologico Monzino, Milan 20138, Italy; [5]Department of Cardiovascular Medicine, Università Cattolica, Rome 00168, Italy; [6]Department of Pediatric Cardiology and Cardiac Surgery, Bambino Gesù Children's Hospital IRCCS, Rome, Italy; [7]San Raffaele Pisana Scientific Institute for Research, Hospitalization and Health Care, 00163 Rome, Italy; and [8]Goethe University, Internal Medicine Clinic III, Frankfurt am Main 60590, Germany

Received 25 November 2015; revised 8 August 2016; accepted 13 August 2016

Time for primary review: 42 days

Aims Beyond the control of nuclear-cytoplasmic trafficking nucleoporins regulate gene expression and are involved in cardiac diseases. Notably, a number of cardiovascular disorders have been linked to alterations in epigenetic mechanisms. Here we aimed to determine the contribution of Nup153 to the epigenetic alterations occurring in cardiomyopathy of dystrophin-deficient *mdx* mice (C57BL/10ScSn-Dmd^{mdx}/J).

Methods and results Nup153 was lysine-acetylated and its expression was significantly increased at protein level in *mdx* hearts compared with controls. Accordingly, lysine acetyl transferase (KAT) activity associated with Nup153 was higher in *mdx* hearts paralleling increased binding with the lysine acetylases P300/CBP-associated factor (PCAF) and p300. Interestingly, Nup153 silencing in *mdx* organotypic heart tissue slices caused a reduction in PCAF- and p300-specific activities. Remarkably, the level of nitric oxide (NO), which is reduced in *mdx* mice, was important for KAT-dependent regulation of Nup153. In fact, treatment of *mdx* heart tissue with an NO donor or the KAT inhibitor anacardic acid normalized Nup153 protein expression. Nup153 was recruited to chromatin and regulated the transcription of genes involved in cardiac remodelling, including the actin-binding protein nexilin. Accordingly, nexilin protein expression was abrogated by Nup153 silencing in *mdx* organotypic cultures. Electrophysiological and molecular experiments revealed that Nup153 overexpression in normal cardiomyocytes increases $Ca_v1.2$ calcium channel expression and function. Alterations in Nup153 protein expression and intracellular localization were also found in dystrophic cardiomyocytes derived from patient-specific induced pluripotent stem cells. Importantly, Nup153 up-regulation and increased acetylation were also found in the heart of Duchenne muscular dystrophy patients.

Conclusions Our data indicate that Nup153 is an epigenetic regulator which, upon altered NO signalling, mediates the activation of genes potentially associated with early dystrophic cardiac remodelling.

Keywords Nucleoporin • Muscular dystrophy • Nitric oxide • Acetylation • Chromatin immunoprecipitation

1. Introduction

Duchenne muscular dystrophy (DMD) is a genetic disease characterized by progressive skeletal and cardiac muscle deterioration caused by mutations of the structural protein dystrophin.[1] Both DMD patients and *mdx* mice (that is an animal model of the disease) develop electrocardiogram abnormalities, impaired conduction, arrhythmias, and dilated cardiomyopathy. Due to improvements in healthcare practices DMD patients live longer and cardiac failure is emerging as a more prevalent cause of death. Downstream of the genetic mutation, several signalling pathways related to nitric oxide (NO), calcium, fibrosis, and immunity are altered and converge on deregulated gene expression.[2] However, how dystrophin

*Corresponding author. Tel: +39 0630154966; fax: +39 0630154665, E-mail: claudia.colussi@cnr.it and Tel: +39 0630154966; fax: +39 0630154665, E-mail: antonella.farsetti@cnr.it

mutations, alterations in the downstream signalling cascades, and aberrant gene expression are linked and lead to cardiomyopathy is not completely understood.

In this context NO deficit, which characterizes DMD and arises as a consequence of NO synthase displacement from the dystrophin complex, is particularly relevant because NO is a key signalling molecule that regulates cardiac function through both vascular-dependent effects and modulation of cardiomyocyte contractility/relaxation. Specifically, NO signalling modulates key factors in the mechanism of excitation–contraction coupling such as the ryanodine receptor and phospholamban thus regulating Ca^{2+} storage in the sarcoplasmic reticulum.[3] Thus, loss of NO signalling strongly affects calcium homeostasis and cardiac function. In addition, NO deficit is associated with mitochondrial dysfunction and increased reactive oxygen species, which contribute to inflammation, fibrosis and finally to cardiomyopathy development. Interestingly, altered NO availability characterizes not only DMD pathology but also many chronic disorders including hypertension and diabetes.[4] To date there are no therapies to safely and effectively restore NO homeostasis because NO release is stimulus-specific, spatially regulated within the cells and further modulated by multiple interacting proteins. Therefore, the identification of NO mediators/downstream effectors may allow therapeutic intervention to prevent cardiac functional decline.

Our previous studies, focused on skeletal muscle, showed that altered NO signalling in *mdx* mice induces a deregulated function of lysine deacetylases (KDACs), unbalanced histone protein acetylation and inhibition of differentiation[3,4] thus providing novel evidence on the epigenetic role of NO. In subsequent studies we found that current spreading in young *mdx* hearts, which do not display an overt clinical manifestation, was negatively regulated by connexin 43 hyperacetylation. This was due to an increase in lysine acetyltransferase (KAT) activity and specifically that of P300/CBP-associated factor (PCAF). These data support the view that early alteration in the function of enzymes regulating protein acetylation levels may affect cardiac function and trigger the development of dystrophic pathology.

Although our data showed that KAT alteration was, at least in part, mediated by oxidative stress, information on the molecular mechanisms linking NO deregulation to KAT function and the effects on target genes is still missing.

Recently, nucleoporins (NUPs), which span the nuclear envelope and control nucleus–cytoplasm transport, have been described as important regulators of gene expression and chromatin structure.[5-7] NUPs are involved in physiological processes such as development and differentiation[8,9] and their dysregulation also emerged as an important determinant in several diseases,[10] including heart dysfunction.[11]

Recent studies revealed an interesting correlation between increased Nup160 and Nup153 protein levels with ventricular function in ischaemic cardiomyopathy whereas other studies identified a number of NUP transcripts, including Nup153, as deregulated in dilated cardiomyopathy.[12]

However, the functional meaning of increased Nup153 during heart ischaemia[8] or its role in DMD cardiomyopathy is currently unknown. Thus, we tested the hypothesis that Nup153 is a mediator of NO-altered signalling driving epigenetic alterations which contribute to the development of dystrophic cardiac dysfunction.

Through different *in vitro* and *in vivo* approaches we established that, following NO deregulation, Nup153 is overexpressed in dystrophic cardiac muscle, is regulated by acetylation and controls a set of genes, such as nexilin (Nexn), versican (Vcan), adrenergic receptor alpha 2a (Adra2), and cAMP responsive element modulator (Crem), involved in cardiac dysfunction. Furthermore, we found evidence that this pathological mechanism translates into induced pluripotent stem cells (iPSC)-derived cardiomyocytes and cardiac biopsies from dystrophic patients.

2. Methods

2.1 HL-1 cardiomyocyte culture and treatments

HL-1 mouse atrial cardiomyocytes were kindly donated by William Claycomb (Louisiana State University, New Orleans) and cultured in complete Claycomb medium.

Cells were treated for 24 h with the following drugs: the NO synthase pan-inhibitors, 7-nitroindazole (7N, 500 μM) or L-NG-nitroarginine methyl ester (LNAME, 5 mM); the KAT inhibitor anacardic acid (AA, 17 μM); hydrogen peroxide (H_2O_2, 100 μM); and actinomycin D (ActD, 0.5 μg/mL). Treatment with the PCAF-specific activator pentadecylidenemalonate1b (SPV106, 25 μM) was performed for 4 h, where indicated cells were treated with LNAME in combination with AA or ActD for 24 h. Nup153 down-regulation was performed by transfecting cells with a mix of three siRNA oligos at 30 nM each (s104224, s104225, s104226; Ambion) in Optimem by siPORT^{TM}NeoFX^{TM} Transfection Agent according to manufacturer's instructions (Thermo Fisher Scientific, Italy). At 48 h post-transfection LNAME was added and samples were incubated for a further 24 h and then collected.

2.2 H9c2 culture, transfection, and cardiac differentiation

H9c2 is a clonal ventricular cardiac cell line isolated from embryonic rat ventricles which is commercially available (SIGMA). Myoblasts were maintained in Dulbecco's modified Eagle's medium (DMEM; Sigma-Aldrich) supplemented with 10% foetal bovine serum, 4 mM L-glutamine, 100 U/mL penicillin, and 100 mg/mL streptomycin. H9c2 myoblasts were transfected with GFP-tagged Nup153 (GFP-Nup153; OriGene) or PINCO-GFP vector as control with lipofectamine 2000 (Invitrogen) according to manufacturer's instructions. Three days after transfection cells were differentiated along the cardiac lineage for 10 days by changing the medium to DMEM supplemented with 1% horse serum and 1 μM retinoic acid (media was renewed every 2 days). Cardiac differentiation was confirmed by analysis of sarcomeric actin expression.

2.3 iPSC-derived cardiomyocytes

iPSCs were generated, fully characterized, differentiated into cardiomyocytes and analysed as reported in the Supplementary material online.

2.4 DMD human patients

Human DMD and control biopsies were obtained from the Bambino Gesù Children's Hospital IRCCS according to the protocol approved by the Ethics Committee of the Hospital and analysed as described in the Supplementary material online.

2.5 Animals

All animal experimental procedures complied with the guidelines of the European Parliament (Directive 2010/63/EU for the protection of laboratory animals) and with the guidelines of the Italian National Institute of Health and were approved by the Institutional Animal Care of Università Cattolica (approval number: 100/2003-A, Rome, Italy). Male 5-month-old C57BL/10ScSnJ (WT) and C57BL/10ScSn-Dmd^{mdx}/J (*mdx*) mice

were used. Mice were randomly divided into groups to receive either AA (5 mg/kg) or the antioxidant compound *N*-acetylcysteine (NAC, 200 mg/kg) or vehicle (DMSO) for 4 days via ip. At the end of treatments animals were anaesthetized by inhalation of 2–5% isofluorane, sacrificed by cervical dislocation, and tissue collected for both histological and biochemical analyses. Atria were removed and both ventricles were used in all analyses. Doses were chosen according to our previous *in vivo* studies.[13,14]

2.6 Heart organotypic culture and infection

WT and *mdx* heart organotypic cultures were prepared and cultured as indicated in the Supplementary material online. This *ex vivo* system allows efficient drug delivery in 300 μm thick ventricle slices while maintaining the physiological cardiac 3D structure.[15] Treatment of slices with the NO donor diethylenetriamine/nitric oxide adduct (DETANO) was performed for 24 h at a concentration of 100 and 500 μM. Lentiviral mediated sh-RNA knockdown for Nup153 was performed using 20 μL of lentivirus (1×10^6 IFU; Santa Cruz Biotechnology sc-41279-V) dissolved in 1 mL of complete 199 medium supplemented with polybrene 5 μg/mL. Control-shRNA-lentiviral-particles (sc-108080) were used as a negative transduction control. Medium was changed 24 h after transduction and samples processed at 72 h post-transduction.

2.7 Western blot and immunoprecipitation

Western blot (WB) analysis and immunoprecipitation were performed according to standard procedures. Method details are described further in the Supplementary material online.

2.8 Patch-clamp recordings

Macroscopic currents flowing through voltage-gated calcium channels were recorded with the patch-clamp technique in the whole-cell configuration as previously described.[16,17] Further methodological details are described in the Supplementary material online.

2.9 Confocal analysis

Heart sections were deparaffinized and microwaved for antigen retrieval in 0.01 M citrate buffer. HL-1, H9c2 cells, or CM-d-hiPSCs were fixed in 4% paraformaldehyde for 10 min and permeabilized (0.1% triton for 10 min). Samples were blocked with 10% bovine serum albumin/PBS, subjected to immunofluorescence as previously described[14] and analysed with a confocal laser scanning system (TCS-SP2; Leica Microsystems). Confocal settings were the same for all examined samples in order to compare fluorescence intensities. Graphics were obtained from the entire stack of images using the 3D plot mode of the Leica TCS-SP2 software. Mean fluorescence intensity was evaluated on the whole stack and corrected for nuclear area. Four to five mice for each group were evaluated and about 200 nuclei were counted in randomly chosen fields by an observer blind to the identity of the samples. Nup153 positive nuclei were expressed as percentage of total nuclei identified by 4′,6-diamidin-2-fenilindolo (DAPI) staining.

2.10 Cardiotoxicity quantitative polymerase chain reaction array

Gene expression analysis was assessed by cardiotoxicity quantitative polymerase chain reaction (qPCR) array (SABiosciences, Qiagen) as indicated in[18] and in the Supplementary material online.

2.11 Chromatin immunoprecipitation

Chromatin immunoprecipitation (ChIP) assays were performed as previously described[3,19,20] using specific antibodies to Nup153 (Santa Cruz, polyclonal), p300 (Santa Cruz, polyclonal) and acetylated histone H3 lysine H3k9Ac (Abcam, monoclonal), normal IgG (Santa Cruz) or no antibody (NoAb) served as negative control. DNA fragments were recovered and analysed by quantitative reverse transcriptase PCR with ABI Prism 7500 PCR instrument as previously described.[3] Nexn, Vcan, CycB1, and Kat8 promoter primer sequences used for ChIP are as in the Supplementary material online and ref 20.

2.12 RNA extraction and real-time PCR analysis

Total RNA was extracted using TRIzol Reagent (Invitrogen) following the manufacturer's instructions. cDNA preparation and real-time PCR conditions were performed as described previously.[19,20] Primer sequences are indicated in the Supplementary material online. For calcium channel analysis, primers and PCR conditions were as in ref 21.

2.13 KAT activity

The KAT assay was performed according to the manufacturer's instructions (Biovision colorimetric kit). HL-1 cells or hearts were homogenized in lysis buffer and 100 μg protein from total extracts was used. Nup153, p300- or PCAF-associated KAT activities were evaluated after immunoprecipitation of the samples with the specific antibodies as described in the Supplementary material online.

2.14 Statistics

Data are expressed as mean of independent experiments ± standard error of the mean (S.E.M.). Significance in normally distributed samples was calculated using a two-tailed *t*-test and one-way analysis of variance (ANOVA) followed by *post hoc* tests [Student–Newman–Keules (SNK)] for multiple comparison. In the other cases non-parametric tests were applied. *P*-values of <0.05 were considered as significant in all tests. For all analyses, the observer was blind to the identity of the samples.

3 Results

3.1 Nup153 protein expression is altered in *mdx* cardiomyocytes and depends on the availability of NO

Evaluation of Nup153 protein expression in *mdx* heart revealed that it was up-regulated compared with normal controls as demonstrated by confocal (*Figure 1A–C*) and western blot analyses (*Figure 1E*). Counterstaining with α-sarcomeric actin was used to provide a better visualization of cardiomyocytes. Consistently, the number of Nup153-expressing nuclei was higher in *mdx* cardiomyocytes than in controls (*Figure 1D*). To check whether the constitutive deficiency of NO that characterizes DMD[22] played a role in the altered Nup153 expression, heart organotypic cultures were treated with the NO donor DETANO (100 or 500 μM) for 24 h. DETANO treatment, at both doses, normalized Nup153 levels in organotypic slices obtained from *mdx* mice (*Figure 1F*). Notably, the 500 μM DETANO treatment also lowered Nup153 protein in normal heart slices (*Figure 1G*). Conversely, reduction of NO by NO synthase inhibitors [LNAME (*Figure 1H, I and 7N*, data not shown)] was sufficient to up-regulate Nup153 protein in HL-1 cardiomyocytes. Evaluation of Nup153 mRNA by qPCR revealed similar levels

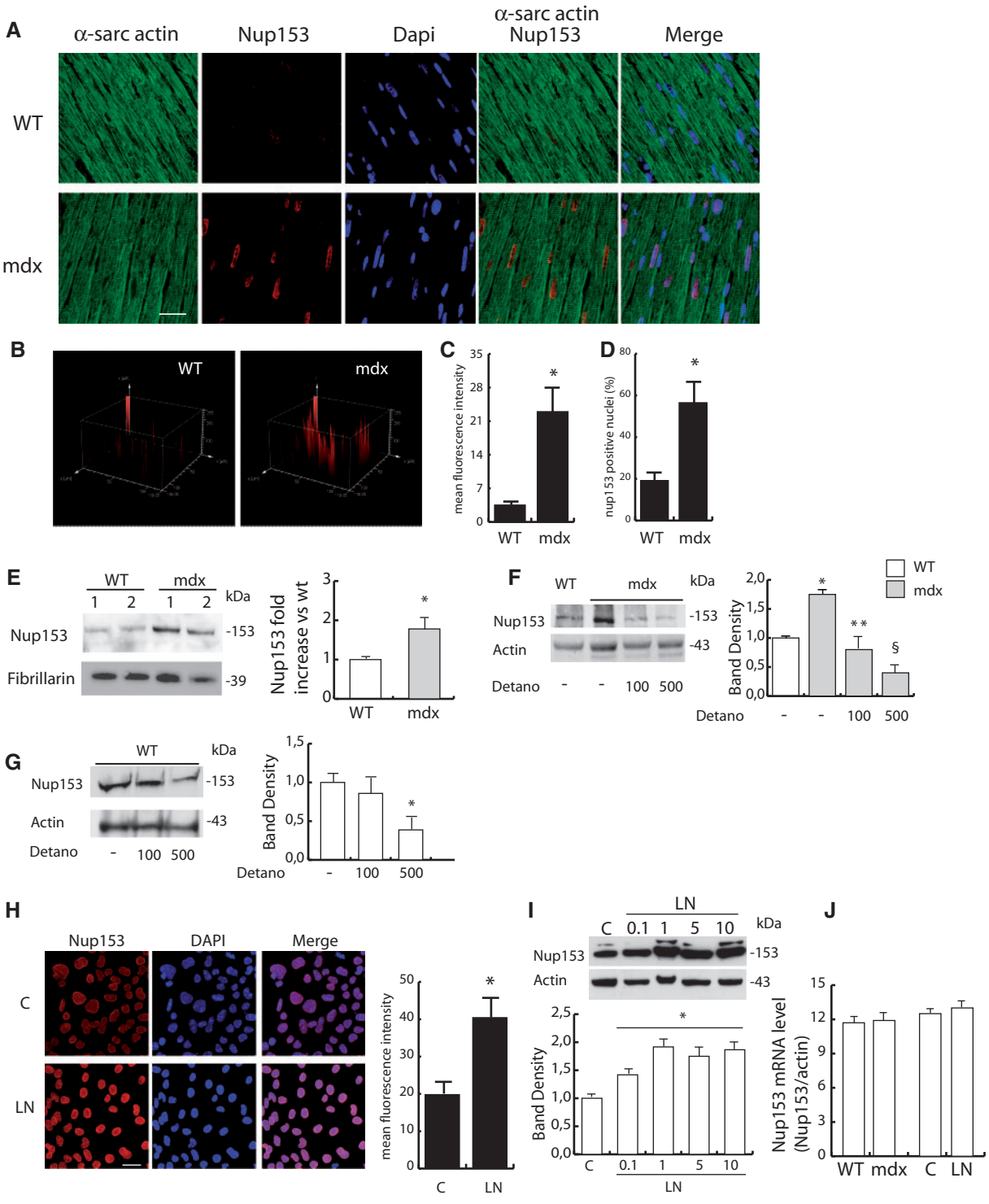

Figure 1 Nup153 protein expression is up-regulated in the *mdx* heart and controlled by NO availability. (*A*) Representative images of Nup153 (red) expression in WT and *mdx* ventricles counterstained with α-sarcomeric actin (green) or with DAPI (scale bar: 20 μm). 3D plots relative to Nup153 expression are shown in (*B*). (*C* and *D*) Mean fluorescence intensities (3.5 ± 0.59 WT vs. 22.9 ± 6.8 *mdx* mice) and the percentage of Nup153^{+} nuclei (22.4 ± 7.8% WT vs. 56.4 ± 12.5% *mdx* mice) in ventricle sections ($n = 4$ control, $n = 5$ *mdx* mice, $^{*}P < 0.01$, *t*-test). (*E*) Nup153 level in WT and *mdx* mice by WB (two representative animals per group are shown) and densitometry (mean fold increase), $^{*}P < 0.05$ vs. *WT*, Mann–Whitney. (*F* and *G*) Nup153 protein level in WT and *mdx* heart organotypic cultures treated or not with DETANO (100, 500 μM for 24 h). The graphs show the densitometry ($^{*}P < 0.01$ vs. WT, $^{**}P < 0.05$ vs. *mdx*, §$P < 0.01$ vs. *mdx*, ANOVA followed by SNK *post hoc*, $n = 5$). (*H*) Representative confocal images showing Nup153 (red) in Hl-1 cells untreated (*C*) or treated with LNAME (LN, 5 mM, 24 h). Nuclei were counterstained with DAPI (scale bar: 50 μm, $n = 4$). Right panel shows the mean fluorescence intensities relative to control and LNAME-treated cells (19.81 ± 3.8 and 40.43 ± 5.8, respectively, $^{*}P < 0.05$ vs. control, *t*-test. (*I*) Nup153 protein level in HL-1 cells treated with LNAME (0.1–1–5–10 mM) for 24 h ($n = 3$). Lower panel shows the densitometric analysis ($^{*}P < 0.05$ vs. control, Kruskal–Wallis on ranks followed by Dunnet *post hoc*). (*J*) Nup153 mRNA levels by qPCR in WT and *mdx* mice ($n = 4$) and in control or LNAME-treated HL-1 ($n = 4$). Independent Hl-1 culture was used.

in WT and *mdx* hearts as well as in LNAME-treated HL-1 cells compared with controls (*Figure 1J*).

3.2 Nup153 levels are regulated by protein acetylation

HL-1 cells were treated with the PCAF activator SPV106 and compared with cells treated with LNAME or H_2O_2. *Figure 2A and B* shows that Nup153 protein level was similarly increased in all these conditions. On the contrary, exposure of HL-1 to the KAT pan-inhibitor AA counteracted Nup153 protein stabilization induced by LNAME (*Figure 2C* and see Supplementary material online, *Figure S1A*). As these data indicated that the modulation of KAT activity affected Nup153 protein level, we tested the hypothesis that protein acetylation might be directly involved in the NO-dependent regulation of Nup153 protein level. Protein immunoprecipitation experiments indicated that, under NO deprivation or in the presence of H_2O_2, Nup153 lysine acetylation was higher than in control conditions (*Figure 2D*). Notably, NO deprivation for 24 h increased the KAT activity *in vitro* (*Figure 2E*, 1.9-fold increase vs. controls).

Consistently, the acetylation level of Nup153 was higher in the hearts of *mdx* mice than in normal controls as demonstrated by IP (*Figure 3A*). This observation was paralleled by an increased association of Nup153 with PCAF and p300 (*Figure 3B*) and an increment of KAT activity specifically associated with Nup153 (*Figure 3C*).

As protein acetylation level is regulated by the balanced activity of KAT and KDAC family members, we also investigated the binding of Nup153 to HDAC5, a Class IIa KDAC which is functionally altered in *mdx* skeletal muscles and known to be activated by NO.[3] Remarkably, in our experimental conditions Nup153–HDAC5 association was reduced in *mdx* hearts (*Figure 3B*).

To investigate the effect of lysine acetylation on the expression of Nup153 protein, *mdx* mice were treated with AA. Western blot analysis showed that Nup153 levels were reduced in *mdx* mice following AA treatment for 4 days (*Figure 3D* and see Supplementary material online, *Figure S1B*). Interestingly, the antioxidant compound NAC produced similar results suggesting that oxidative stress contributed to the stabilization of Nup153 protein (see Supplementary material online, *Figure S1B*).

Remarkably, KAT basal activity, which was elevated in *mdx* hearts, was partially reduced when Nup153 was down-regulated by sh-Nup153 lentivirus transduction in the organotypic culture system (*Figure 3E*). Similarly, PCAF- and P300-specific KAT activities were decreased in Nup153-silenced *mdx* samples in comparison to *mdx* (*Figure 3F and G*).

3.3 Nup153 regulates genes involved in cardiac remodelling

To understand the putative role of Nup153 as regulator of gene expression in response to NO deficit, Nup153 was silenced in HL-1 cells in the presence or absence of LNAME (24 h treatment) and the expression of 84 key genes involved in cardiac injury was profiled by a qPCR array. In this experiment, LNAME induced an up-regulation of a specific sub-set of genes (37/84 genes; $P < 0.05$) that was counteracted by Nup153 silencing (36/37 genes), suggesting that Nup153 is a positive gene modulator during NO deprivation (see cluster, Supplementary material online, *Figure S2A*). The LNAME- and Nup153-dependent regulation of selected genes including Nexn, Adra2, and Vcan was further validated by qPCR in independent sample preparations (see Supplementary material online, *Figure S2B* and *C*).

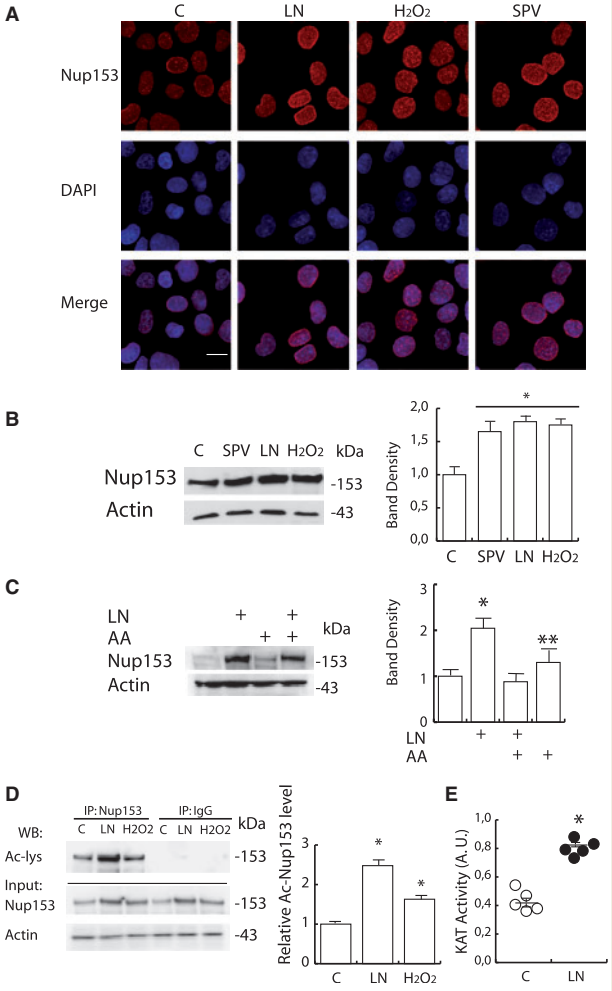

Figure 2 Nitric oxide deprivation increases KAT activity and Nup153 acetylation in HL-1 cells. (*A*) Confocal analysis of Nup153 in HL-1 cells untreated (*C*) or treated with LNAME (LN, 5 mM, 24 h), H_2O_2 (100 μM, 24 h), or the PCAF-specific activator SPV106 (SPV; 25 μM, 4 h). Nuclei were counterstained with DAPI (scale bar: 50 μm) ($n = 4$). (*B*) Western blot showing Nup153 protein levels in HL-1 cells in the above conditions and densitometry analysis [$^*P < 0.05$ vs. control, *t*-test ($n = 4$)]. (*C*) Nup153 level in HL-1 treated with LNAME alone or in combination with the KAT pan-inhibitor AA (17 μM, 24 h) ($n = 3$). Densitometry is shown in the right panel, $^*P < 0.05$ LN vs. control, $^{**}P < 0.05$ LN vs. LN/AA, ANOVA followed by SNK *post hoc*. (*D*) Analysis of Nup153 acetylation level in untreated HL-1 or under NO deprivation by LNAME or oxidative stress by IP. The graph shows acetylated Nup153 level relative to input ($n = 5$) $^*P < 0.05$ vs. control, Kruskal–Wallis on ranks followed by SNK *post hoc*. (*E*) KAT activity in LNAME-treated or control HL-1 cells (0.42 ± 0.037 control vs. 0.83 ± 0.027 LN-treated cells, mean ± S.E.M., $n = 5$, $^*P < 0.01$ vs. control, ANOVA, A.U. Arbitrary Units). Independent Hl-1 culture was used.

Additional experiments revealed that the LNAME-dependent increase in Nexn transcript was abrogated by co-treatment with the transcription inhibitor ActD (*Figure 4A*). Although recent data indicate that Nup153 may associate with actively transcribed genomic regions in

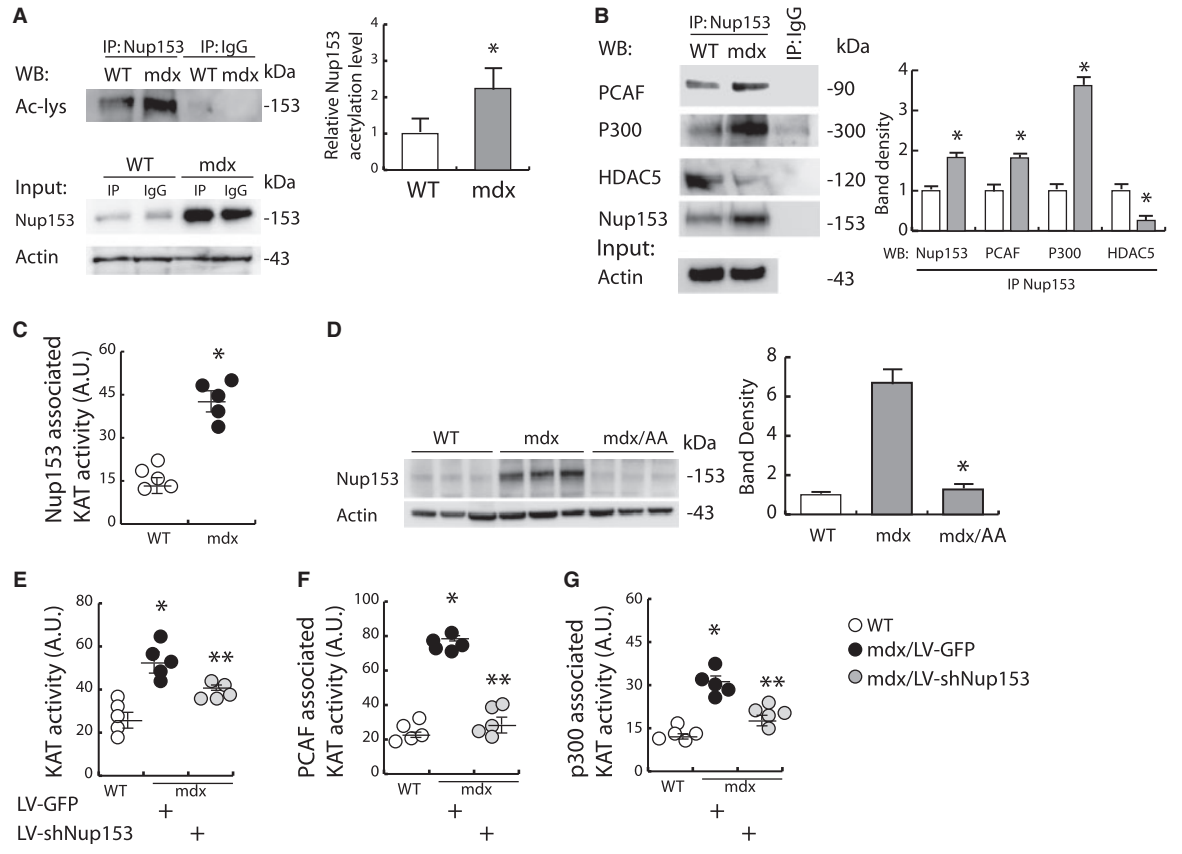

Figure 3 Nup153 is acetylated and associated with KATs in the *mdx* heart. (*A*) Analysis of Nup153 acetylation level by IP in WT and *mdx* hearts. The graph shows acetylated Nup153 level relative to input ($n = 5$, $^{*}P < 0.01$ vs. WT, Mann–Whitney Rank Sum Test). (*B*) Co-IP showing Nup153 association with p300, PCAF, and HDAC5 in extracts from WT and *mdx* hearts. Densitometric analysis is shown in the right panel ($n = 3$). (*C*) Evaluation of Nup153 associated KAT activity in WT and *mdx* hearts (14.6 ± 2 WT vs. 44.4 ± 3.3 *mdx*, $n = 5$ $^{*}P < 0.01$ vs. WT, *t*-test). (*D*) Western blot showing Nup153 levels in WT and *mdx* mice treated with AA or vehicle control. Densitometry analysis is shown in the graph ($n = 3$, $^{*}P < 0.05$ vs. *mdx*, ANOVA followed by SNK *post hoc*). (*E–H*) KAT activity in extracts from WT and *mdx* organotypic cultures transduced with GFP-control or sh-Nup153 lentiviral particles for 72 h in basal conditions (25.6 ± 3.75 WT, 54.4 ± 3.93 *mdx*/LV-GFP, 38.6 ± 1.86 *mdx*/LV-shNup153, $^{*}P < 0.05$ vs. WT, $^{**}P < 0.05$ vs. *mdx*/LV-GFP) (*E*) and after IP for PCAF (21.2 ± 2.7 WT, 78 ± 2 *mdx*/LV-GFP, 28.12 ± 4.19 *mdx*/LV-shNup153, $^{*}P < 0.05$ vs. WT, $^{**}P < 0.05$ vs. *mdx*/LV-GFP) (*F*), and p300 (10.88 ± 1.1 WT, 30.6 ± 2.1 *mdx*/LV-GFP, 18.6 ± 1.6 *mdx*/LV-shNup153, $^{*}P < 0.05$ vs. WT, $^{**}P < 0.05$ vs. *mdx*/LV-GFP) (*G*) ($n = 5$, mean ± S.E.M., ANOVA followed by SNK *post hoc*).

Drosphila,[23] the chromatin binding of Nup153 to specific genes has not been demonstrated in mammals yet. In this context, ChIP experiments showed that the recruitment of Nup153 to chromatin and the acetylation of histone H3 lysine 9 (H3k9ac) was increased on Vcan and Nexn promoters in the presence of LNAME (*Figure 4B*) as well as on the K(lysine) acetyltransferase 8 (Kat8) promoter which acted as a positive control (*Figure 4C*).[24] CycB1, whose mRNA was not modulated by LNAME (*Figure 4D*), was used as a negative ChIP control. On this promoter, a similar Nup153 recruitment and H3k9ac enrichment occurred in control and LNAME-treated HL-1 cells (*Figure 4C*). Accordingly, LNAME treatment significantly increased Nexn mRNA levels (*Figure 4D*). Notably, Nup153 silencing (*Figure 4E*) reduced Nexn protein basal levels, prevented the LNAME-dependent Nup153 protein increase, and counteracted nexilin protein up-regulation (*Figure 4F*). Similar results were obtained with versican, another Nup153-regulated gene identified by *in vitro* screening (see Supplementary material online, *Figure S3*).

RNA expression analysis of Vcan, Crem, Adra2, and Nexn showed that these genes were up-regulated in the hearts of dystrophic mice compared with controls (*Figure 5A*). In *mdx* hearts, confocal microscopy revealed that, in association to the increased protein levels, nexilin was characterized by an irregular distribution along sarcomeres (*Figure 5B*). Interestingly, the uneven distribution of nexilin in *mdx* hearts paralleled two other sarcomeric proteins actinin and myosin heavy chain (*Figure 5B*).

To assess the capability of Nup153 to transcriptionally regulate Nexn expression in *mdx* hearts, we performed ChIP experiments. *Figure 5C* shows that in *mdx* hearts Nup153 was present on the Nexn promoter concurrently with the recruitment of p300 on the same region. Analysis of control genes revealed, as expected, that Nup153 binding to the Kat8 promoter[24] was higher in *mdx* hearts, whereas binding to the CycB1 promoter was at similar levels in WT and *mdx* hearts (*Figure 5C*). To address whether Nup153 could have a functional role in Nexn gene expression, organotypic slices of *mdx* hearts were infected with a sh-Nup153 lentiviral vector to down-regulate the protein or a GFP-control lentivirus and analysed 72 h later. The integrity and viability of the cardiac slices, evaluated by cardiac protein expression and metabolic activity,

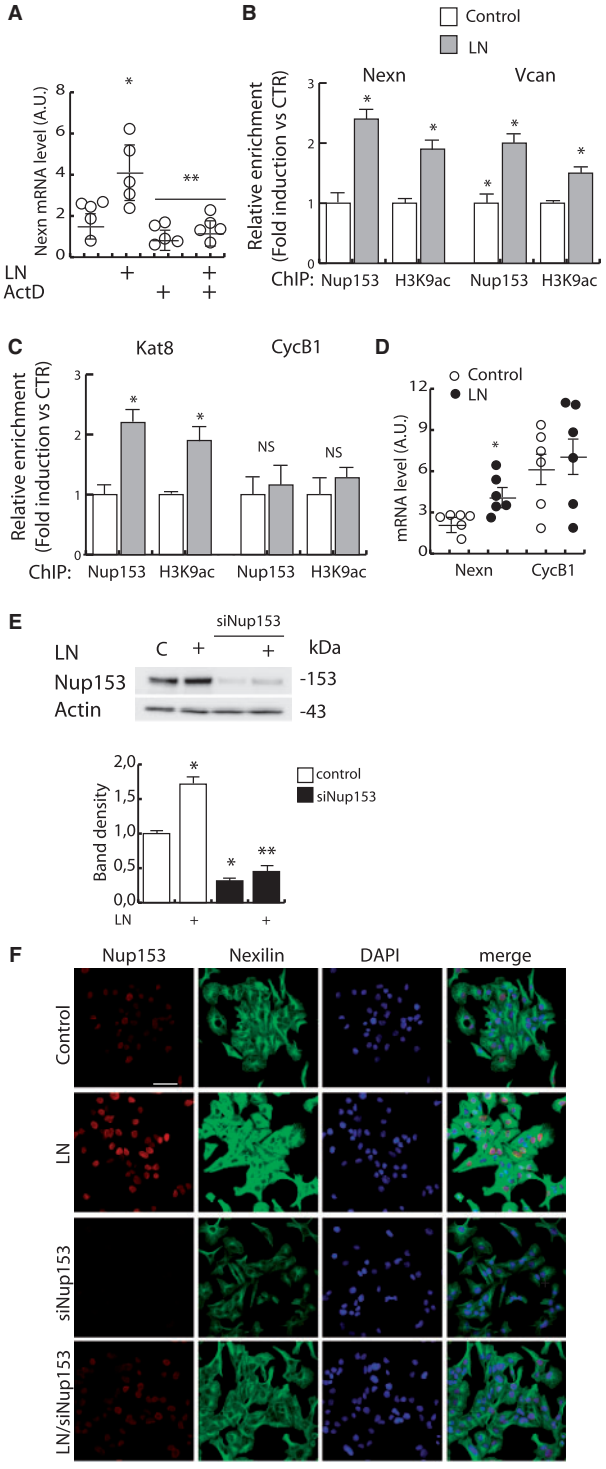

Figure 4 Nup153 transcriptionally regulates Nexn expression in response to nitric oxide signalling in HL-1 cells. (*A*) Nexn mRNA level by qPCR in HL-1 treated with LNAME alone or in combination with actinomycin D (0.5 μg/mL, 24 h) (1.83 ± 0.38, 4.08 ± 0.78, 0.74 ± 0.23 and 1.1 ± 0.28 untreated, LNAME, ActD and LNAME/ActD, respectively), $n = 5$, $^{*}P < 0.05$ vs. control, $^{**}P < 0.01$ vs. LNAME, ANOVA followed by SNK *post hoc*; A.U., Arbitrary Units. (*B* and *C*) ChIPs on HL1 cells treated with or without LNAME showing Nup153 binding and acetylation on histone H3 lysine 9 (H3K9ac) on Vcan and Nexn promoters (*B*) or on Kat8 and CycB1 promoters (*C*) ($n = 5$, $^{*}P < 0.05$ vs. control, ANOVA). (*D*) Nexn and CycB1 mRNA levels (1.9 ± 0.31 vs. 4.02 ± 0.63 and 6.3 ± 1.2 vs. 7.2 ± 1.7, respectively) assessed by qPCR, in control and LNAME-treated HL-1 cells ($n = 6$, $^{*}P < 0.05$ vs. control, ANOVA). (*E*) Representative western blot showing Nup153 silencing in HL-1 treated or not with LNAME for 24 h. The graph shows densitometry analysis ($n = 5$, $^{*}P < 0.05$ vs. control, $^{**}P < 0.05$ vs. LNAME, ANOVA followed by SNK *post hoc*). (*F*) Representative images showing Nup153 (red) and Nexilin (green) proteins in HL-1 cells treated with siRNA for Nup153 or scramble oligos (72 h), alone or in combination with LNAME (24 h, $n = 3$). Nuclei were counterstained with DAPI (scale bar 50 μm). Independent Hl-1 culture was used.

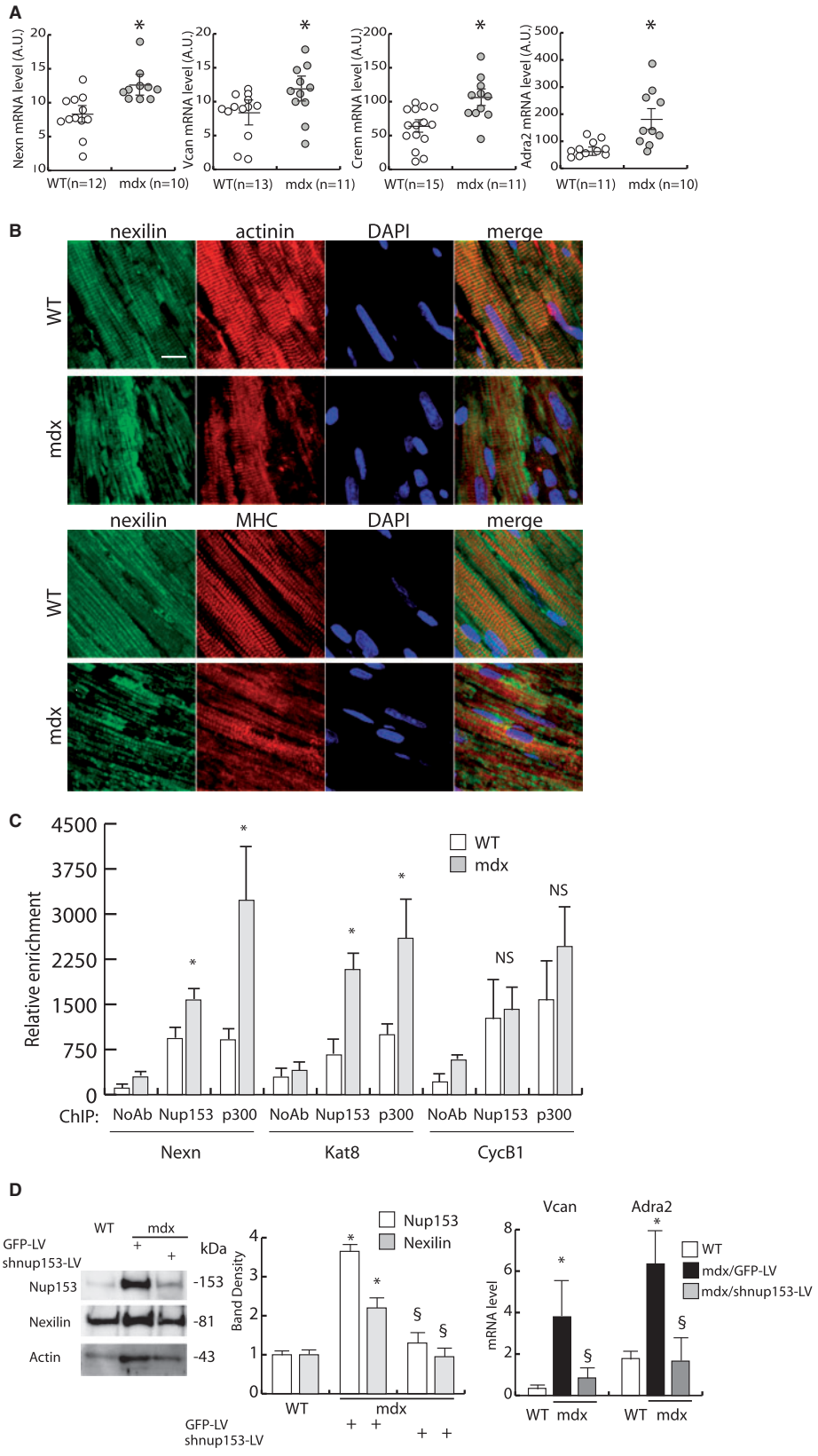

Figure 5 Nup153 transcriptionally regulates Nexn expression *in vivo*. (*A*) mRNA evaluation of Nexn (7.8± 1 WT vs. 12.6 ± 0.9 *mdx*, **P* < 0.05), Vcan (8 ± 1.1 WT vs. 11.4 ± 1.39 *mdx*, **P* < 0.05), Crem (56 ± 8.4 WT vs. 102± 11.3 *mdx*, **P* < 0.05), and Adra2 (53 ± 11.1 WT vs. 167 ± 40.4 *mdx*, **P* < 0.05) in WT and *mdx* hearts by qPCR (sample size and mean are indicated in the figure, ANOVA). (*B*) Panels show representative images of Nexilin expression and distribution in WT and *mdx* ventricle sections co-immunostained either with actinin (upper panels) or with MHC (lower panels). Nuclei were counter-stained with DAPI (scale bar: 10 μm). (*C*) ChIP showing Nup153 and p300 recruitment on Nexn, Kat8, and CycB promoters in WT and *mdx* hearts ($n = 6$, **P* < 0.05 vs. WT, *t*-test); signal from No antibody is also shown (NoAb). (*D*) Nup153 and Nexilin protein levels (left panel) or Vcan and Adra2 mRNA expression (right panel) in organotypic culture from WT and *mdx* hearts transduced with GFP-control or sh-Nup153 lentiviral particles ($n = 3$, **P* < 0.05 vs. WT, §*P* < 0.05 vs. *mdx*/LV-GFP, ANOVA followed by SNK *post hoc*).

was well preserved at this time point (see Supplementary material online, *Figure S4*). In Nup153-silenced *mdx* organotypic cultures, nexilin protein was reduced to normal levels (*Figure 5D*). Consistently, Vcan and Adra2 mRNA expressions, which were up-regulated in *mdx* hearts, were normalized after Nup153 sh-interference in organotypic cultures. These observations lend further supporting evidence of a positive transcriptional regulatory role for Nup153 in dystrophic hearts (*Figure 5D*).

3.4 Nup153 overexpression increases the expression and function of voltage-gated calcium channels

To determine the effects of Nup153 on voltage-gated calcium (Ca_v)1 channels in the absence of other alterations that characterize *mdx* cardiomyocytes, macroscopic Ba^{2+} currents were measured in embryonal ventricular H9c2 cells differentiated towards the cardiac phenotype and overexpressing either a Nup153-GFP vector or an empty-GFP vector (*Figure 6A*). Cells overexpressing Nup153, identified by fluorescent microscopy, showed increased total Ba^{2+} current densities at 0 mV (*Figure 6B and C*) compared with GFP^+ cells suggesting that Nup153 increased high-voltage-activated (HVA) Ca^{2+} currents. To determine the effect of Nup153 on Ca_v1 channels, Ba^{2+} currents were recorded before and after the application of 5 μM nifedipine (a calcium channel blocker). As shown in *Figure 6B and C*, the Ca_v1 current was increased in Nup153 overexpressing cells compared with GFP controls. Electrophysiological findings were supported by western blot analysis showing increased expression of the cardiac α_{1C} subunit of the heteromeric $Ca_v1.2$ channels in H9c2 cells overexpressing Nup153 (*Figure 6D*). As electrophysiological recordings showed a nifedipine-resistant HVA current, we performed PCR experiments in differentiated and proliferating H9c2 cells to determine the expression of α_1 subunit mRNAs from different HVA channels that could potentially contribute to the recorded currents. We found, however, that H9c2 cells only expressed α_{1C} ($Ca_v1.2$) subunit mRNA whereas α_{1A} ($Ca_v2.1$) and α_{1B} ($Ca_v2.2$) mRNAs were not found (see Supplementary material online, *Figure S5*). Although these cells also expressed the α_{1G} ($Ca_v3.1$) subunit, no detectable low-voltage-activated (LVA) current was recorded under this experimental condition suggesting that no 'functional' LVA channels are expressed.

3.5 Nup153 is altered in dystrophic CMs-d-iPSC and in cardiac biopsies from DMD patients

To investigate whether alterations in Nup153 expression and function occur in human cardiomyocytes from Duchenne (DMD) and Becker (BMD) patients, we took advantage of iPSC technology. Specifically, dystrophic and control cardiomyocytes were successfully derived from iPSCs (CMs-d-iPSCs), as evidenced by positive cardiac troponin T type 2 staining (*Figure 7A* and see Supplementary material online, *Figure S6A*), while maintaining a dystrophic phenotype as assessed by dystrophin expression and evaluation of the percentage of abnormal nuclei, that is a cell death marker associated with dystrophic cardiac disease[25] (see Supplementary material online, *Figure S6B–D*). *Figure 7B* shows that Nup153 protein is expressed at higher levels in both DMD and BMD CMs-d-iPSCs compared with control CMs-d-iPSCs. Interestingly, the CMs-d-iPSCs obtained from BMD revealed the highest increase in total Nup153 expression paralleled by a diffuse nucleoplasmic localization (*Figure 7C and D*). Additional experiments performed on cardiac biopsies revealed that DMD patients, with cardiac dysfunction, showed very high levels of Nup153 protein and uneven nexilin intracellular distribution compared with non-dystrophic controls as assessed by confocal analysis (*Figure 7E*). In a separate set of control and DMD patients, we confirmed this trend regarding the overexpression of Nup153 and nexilin by western blot and increased levels of acetylated Nup153 by IP (*Figure 7F and G*).

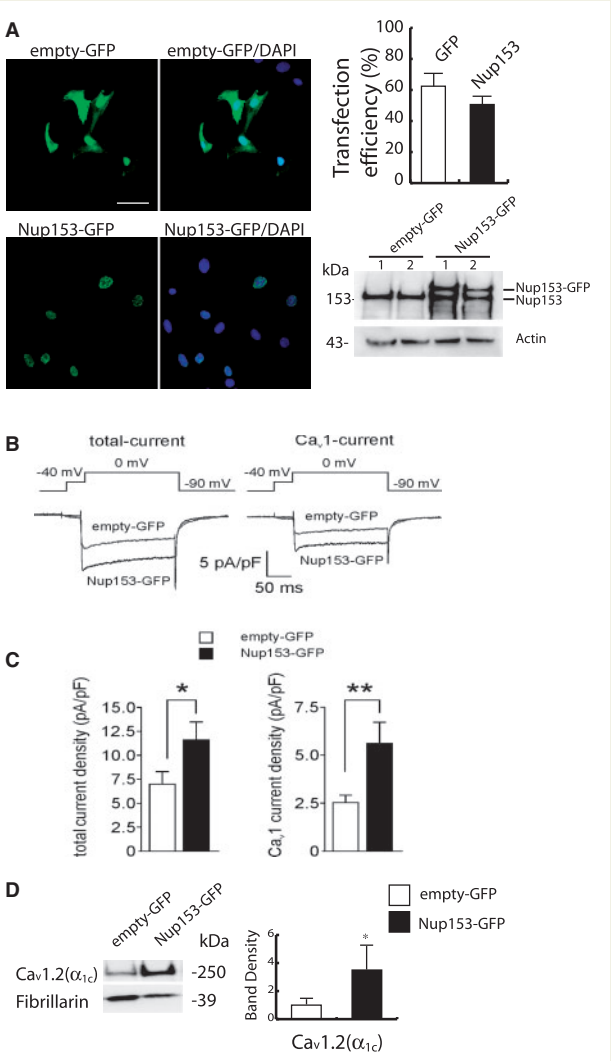

Figure 6 Nup153 overexpression increases Ca_v channel expression and function. (*A*) Differentiated H9c2 cells expressing either a GFP-tagged Nup153 or an empty-GFP vector, as control, analysed by western blot (anti-Nup153 antibody recognizes both the endogenous and the slower migrating overexpressed GFP-tagged Nup153 protein) or by immunofluorescence. Nuclei were counterstained with DAPI (scale bar 50 μm). The graph shows the percentage of transfection in the two conditions. (*B*) Representative traces of total (left panel) and nifedipine-sensitive Ba^{2+} current density (right panel) in control-GFP and Nup153-overexpressing H9c2 cells; (*C*) Mean total and Ca_v1 current density in GFP or Nup153 overexpressing cells ($n = 20$, $^*P < 0.05$ $^{**}P < 0.01$, *t*-test). (*D*) Western blot showing $Ca_v1.2$ α_{1C} subunit protein levels in H9c2 cells overexpressing either GFP-tagged Nup153 or empty-GFP vectors. The graph shows the band densities ($n = 3$, $^*P < 0.05$ vs. empty-GFP, *t*-test).

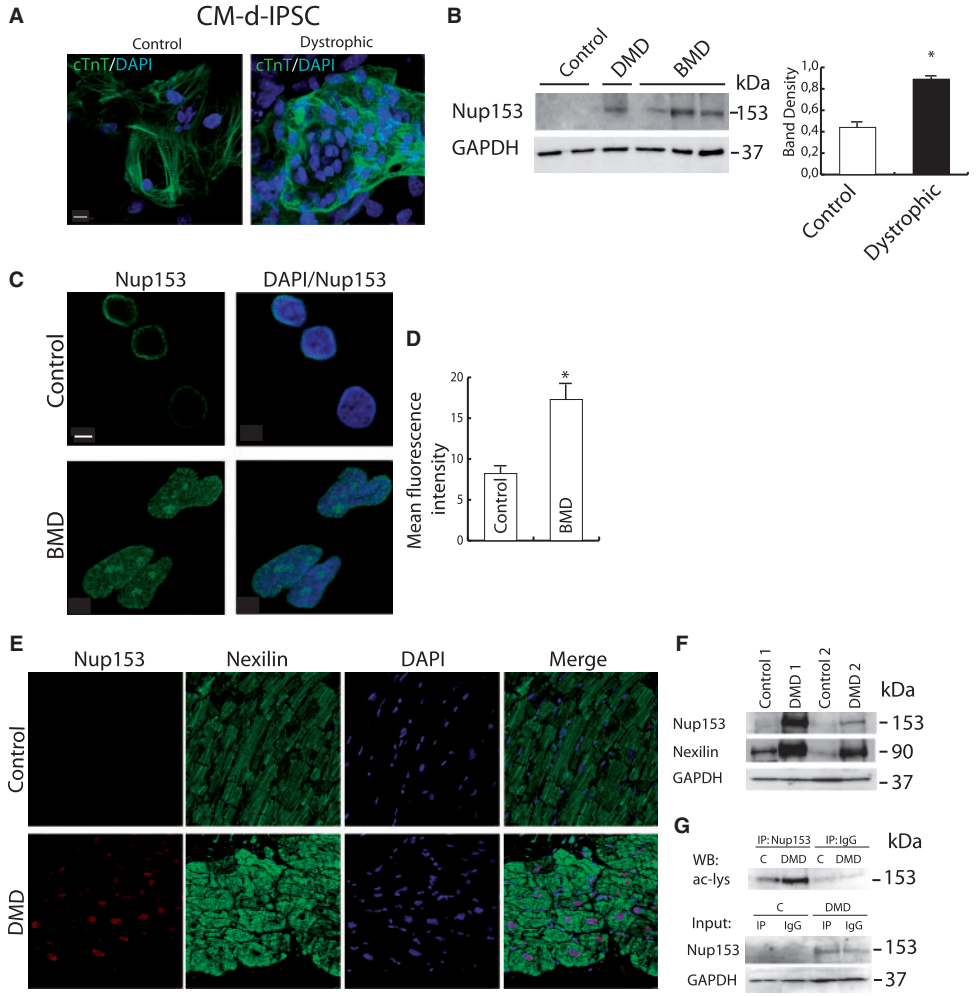

Figure 7 Nup153 expression is altered in CMs-d-iPSC and in heart biopsies from dystrophic patients. (*A*) Representative images of control and BMD CMs-d-iPSC expressing cardiac Troponin T (cTnT, scale bar: 10 μm). (*B*) Western blot showing Nup153 expression in controls (two clones), DMD (one clone), and BMD (three clones) and densitometry (mean ± S.E.M. from controls and dystrophic patients normalized vs. GAPDH, 0.44 ± 0.06 vs. 0.89 ± 0.03, respectively, $^*P < 0.01$, *t*-test). (*C*) Representative images of control and BMD CMs-d-iPSC expressing Nup153 (scale bar: 5 μm) and (*D*) the relative mean fluorescence intensity (8.22 ± 1.38 control vs. 17.29 ± 2.10 BMD, $^*P < 0.05$, *t*-test). (*E*) Representative images showing Nup153 (red) and nexilin (green) expression in heart tissue samples from control ($n = 5$) and DMD patients ($n = 3$). Nuclei were counterstained with DAPI. Scale bar: 20 μm. (*F*) WB showing Nup153 and nexilin levels in control and DMD heart tissue lysates ($n = 2$). (*G*) Representative IP showing Nup153 acetylation level in control and DMD patients ($n = 2$).

4 Discussion

This work provides novel insights into epigenetic mechanisms regulated by NO in the dystrophic heart. In particular, we found that NO-altered signalling affected Nup153 function inducing its association with the lysine acetylases PCAF and p300. Consequently, Nup153 was hyperacetylated in the dystrophic heart imparting important consequences on gene expression possibly through the formation of Nup153-dependent chromatin binding complexes on target promoters. These key findings are summarized in *Figure 8*.

4.1 Novel mechanism of Nup153 regulation in *mdx* hearts

A proteomic study previously identified several nuclear transport proteins, including Nup153, as target of acetylation in a number of cancer cell lines.[26] Here we report, for the first time, that this post-translational modification regulates Nup153 protein level in response to NO and oxidative stress. Importantly, acetylation of non-histone proteins, such as transcription factors and co-activators/repressors may regulate their protein stability/degradation, DNA-binding affinity, the transactivation potential, and interactions in the macromolecular complexes relevant for pathophysiological processes.[27]

It is worth noting that Nup153 silencing significantly reduced PCAF- and p300-specific activities suggesting the presence of a bidirectional regulatory mechanism. Thus, in addition to being an acetylation substrate, Nup153 may play a role in the functional regulation of these epigenetic enzymes. Overall, stress-mediated Nup153 changes may sustain the ongoing aberrant epigenetic mechanisms which characterize the dystrophic heart. Although our data provide novel insights into the importance of acetylation in Nup153 protein regulation, we cannot exclude that

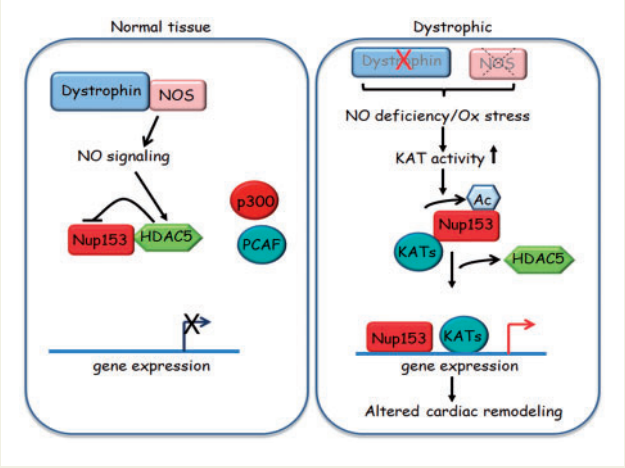

Figure 8 Cartoon illustrating the proposed role of Nup153 in dystrophic heart. In the healthy heart, NO signalling maintains low level of acetylated Nup153 favouring Nup153–HDAC5 interaction and reducing the downstream target gene activation. In the dystrophic heart, NO-altered signalling affects Nup153 function inducing its association with the lysine acetylases PCAF and p300 and increasing its acetylation level. In this context, Nup153-regulated complexes may control pathological gene expression possibly through the binding on target promoters (Nexn, Crem, Adra2, Vcan).

other mechanisms may coexist. In fact, Nup153 has also been shown to be regulated by miR-155[28] as well as by post-translational modifications such as SUMOylation[29] and phosphorylation.[30]

4.2 Role of Nup153 on cardiac gene expression

Although the regulatory role of NUPs on gene expression is well established, at least for cell cycle and developmental genes, less clear points are how they bind to the specific gene loci and which are the co-factors mediating this function.

Several lines of evidence in yeast indicated that chromatin association with NUPs can be mediated by KATs.[31] Our experimental observations showed that KATs are indeed binding partners of Nup153 in the heart of dystrophic mice and that these proteins co-exist on the same promoter regions, thus providing important information on gene regulatory mechanisms. Remarkably, the expression of Vcan, Adra2, Nexn, and Crem, genes implicated in cardiac function regulation, was deregulated in the presence of acetylated Nup153 in 5-month-old *mdx* mice lacking clinically relevant cardiomyopathy manifestations. Although the contribution of these genes to dystrophic cardiomyopathy is to date unknown, our findings suggest that early alteration of these genes could indeed trigger a pathological programme of cardiac remodelling. In fact, Vcan, a major component of the extracellular matrix, plays a central role in tissue morphogenesis and is involved in the transition from acute and chronic cardiac damage to ischaemic cardiomyopathy.[32] Alpha-adrenergic receptors, such as Adra2, are G-protein-coupled receptors activated by catecholamines, whose activation in cardiomyocytes affects intracellular Ca^{2+} reuptake by the sarcoplasmic reticulum Ca^{2+}-ATPase thus influencing cardiac contractility.[33] The overexpression of the transcription factor Crem, which regulates transcription in response to cAMP and other signalling pathways,[34] leads to Ryanodine receptor-mediated calcium leak and atrial fibrillation.[35] Finally, the altered expression and distribution of a sarcomeric-associated protein such as nexilin, whose mutations are involved in both hypertrophic and dilated cardiomyopathy,[36,37] may contribute to the progressive myofibrillar disarray and derangement which lead to cardiac functional impairment in DMD.

4.3 Nup153 and calcium channel function

Multiple alterations co-exist in dystrophic cardiomyocytes all affecting calcium handling.[38] Our data performed in H9c2 cardiomyocytes overexpressing Nup153 clearly identified a role for the protein in the regulation of the expression and function of Ca_v1 (i.e. L-type) channels. These findings may provide at least one mechanism for dystrophin-related calcium channel abnormalities which are at the basis of arrhythmias. Of note, we also found that this cell line which is of embryonic origin showed a nifedipine-insensitive HVA current that we attributed to a nifedipine-resistant Ca_v1 channel isoform. Indeed, these channels have been shown to be developmentally regulated and expressed in neonatal ventricular rat cardiomyocytes, such as H9c2, and in adult cardiomyocytes undergoing dedifferentiation *in vitro*.[39]

4.4 Validation in human patients

It is remarkable that increased Nup153 protein expression and acetylation as well as an altered nexilin level and distribution could be found in human DMD biopsies. Consistently, the Nup153 deregulation characterized in human CMs-d-iPSC generated from both BMD and DMD dystrophic patients highlighted the presence of a cell-autonomous defect associated with dystrophin deficiency. However, there is evidence suggesting that cardiac dysfunction may be more pronounced in BMD patients due to increased demands upon the heart caused by longer ambulation times and the ability of shorter dystrophin isoforms to partially substitute for full-length dystrophin in BMD.[40,41] Thus, our results showing higher levels of Nup153 in BMD CMs compared with those of DMD CMs are remarkable as it may provide evidence of a cardiomyocyte-associated pathophysiological mechanism more pronounced in BMD. However, caution should be used when interpreting these data because a limited number of samples was available for analysis. Future experiments including more patients' samples will be necessary in order to explore this hypothesis in greater detail.

4.5 Study considerations and conclusions

Although further investigations are required to better link the gene expression deregulation to the pathological outcome in human and mice models, and to understand whether direct Nup153 modulation may prevent cardiac dysfunction, our data suggest that Nup153, controlling the expression of genes implicated in cardiac contractility and/or calcium handling, may have a role in the onset of the deterioration of dystrophic heart function.

In summary, this work indicates Nup153 as a sensor of the altered NO signalling pathway with important epigenetic consequences for gene expression in the dystrophic heart. The evidence that NO can regulate Nup153 level also in normal hearts and that Nup153 is altered in other cardiac pathologies[12] characterized by NO deficit suggests that this protein is a broad mediator of NO signalling and oxidative stress. Consequently, Nup153 may represent a valuable therapeutic target for all cardiac diseases related to NO dysfunction not limited to muscular dystrophy.

Supplementary material

Supplementary material is available at *Cardiovascular Research* online.

Acknowledgements

We thank Silvia Bacchetti for critical reading of manuscript, Vera Vigorelli for technical assistance in iPSC culture, Egidio Stigliano for technical assistance in histology, and Viviana Meraviglia for fibroblast isolation from dystrophic patients.

Conflict of interest: none declared.

Funding

This study was supported by the Italian Ministry of Health and the Italian Ministry of Education, University and Research (GR 2011-02351557 and FIRB-MIUR RBFR10URHP_002 to S.N. and RF2010-2318330 and MIUR-PRIN2010TYCL9B_006 to A.F.); Association Française Contre les Myopathies (AFM-TELETHON #18243) to C.C. A.R. is supported by AIRC fellowship. A.G. is funded by a Fondazione Umberto Veronesi Postdoctoral fellowship 2014–2015.

References

1. Finsterer J, Cripe, L. Treatment of dystrophin cardiomyopathies. *Nat Rev Cardiol* 2014;**11**:168–179
2. Tian L, Cao J, Deng X, Zhang C, Qian T, Song X, Huang B. Unveiling transcription factor regulation and differential co-expression genes in Duchenne muscular dystrophy. *Diagn Pathol* 2014;**9**:210.
3. Colussi C, Gurtner A, Rosati J, Illi B, Ragone G, Piaggio G, Moggio M, Lamperti C, D'Angelo G, Clementi E, Minetti G, Mozzetta C, Antonini A, Capogrossi MC, Puri PL, Gaetano C. Nitric oxide deficiency determines global chromatin changes in Duchenne muscular dystrophy. *Faseb J* 2009;**23**:2131–2141.
4. Colussi C, Mozzetta C, Gurtner A, Illi B, Rosati J, Straino S, Ragone G, Pescatori M, Zaccagnini G, Antonini A, Minetti G, Martelli F, Piaggio G, Gallinari P, Steinkuhler C, Clementi E, Dell'Aversana C, Altucci L, Mai A, Capogrossi MC, Puri PL, Gaetano C. HDAC2 blockade by nitric oxide and histone deacetylase inhibitors reveals a common target in Duchenne muscular dystrophy treatment. *Proc Natl Acad Sci U S A* 2008;**105**:19183–19187.
5. Kalverda B, Pickersgill H, Shloma VV, Fornerod M. Nucleoporins directly stimulate expression of developmental and cell-cycle genes inside the nucleoplasm. *Cell* 2010;**140**:360–371.
6. D'Angelo MA, Gomez-Cavazos JS, Mei A, Lackner DH, Hetzer MW. A change in nuclear pore complex composition regulates cell differentiation. *Dev Cell* 2012;**22**:446–458.
7. Dickmanns A, Kehlenbach RH, Fahrenkrog B. Nuclear pore complexes and nucleocytoplasmic transport: from structure to function to disease. *Int Rev Cell Mol Biol* 2015;**320**:171–233.
8. Tarazon E, Rivera M, Rosello-Lleti E, Molina-Navarro MM, Sanchez-Lazaro IJ, Espana F, Montero JA, Lago F, Gonzalez-Juanatey JR, Portoles M. Heart failure induces significant changes in nuclear pore complex of human cardiomyocytes. *PLoS One* 2012;**7**:e48957.
9. Palancade B, Doye V. Sumoylating and desumoylating enzymes at nuclear pores: underpinning their unexpected duties? *Trends Cell Biol* 2008;**18**:174–183.
10. Kehat I, Accornero F, Aronow BJ, Molkentin JD. Modulation of chromatin position and gene expression by HDAC4 interaction with nucleoporins. *J Cell Biol* 2011;**193**:21–29.
11. Molina-Navarro MM, Trivino JC, Martinez-Dolz L, Lago F, Gonzalez-Juanatey JR, Portoles M, Rivera M. Functional networks of nucleocytoplasmic transport-related genes differentiate ischemic and dilated cardiomyopathies. A new therapeutic opportunity. *PLoS One* 2014;**9**:e104709.
12. Omar SA, Webb AJ, Lundberg JO, Weitzberg E. Therapeutic effects of inorganic nitrate and nitrite in cardiovascular and metabolic diseases. *J Intern Med* 2016;**279**:315–336.
13. Colussi C, Berni R, Rosati J, Straino S, Vitale S, Spallotta F, Baruffi S, Bocchi L, Delucchi F, Rossi S, Savi M, Rotili D, Quaini F, Macchi E, Stilli D, Musso E, Mai A, Gaetano C, Capogrossi MC. The histone deacetylase inhibitor suberoylanilide hydroxamic acid reduces cardiac arrhythmias in dystrophic mice. *Cardiovasc Res* 2010;**87**:73–82.
14. Colussi C, Rosati J, Straino S, Spallotta F, Berni R, Stilli D, Rossi S, Musso E, Macchi E, Mai A, Sbardella G, Castellano S, Chimenti C, Frustaci A, Nebbioso A, Altucci L, Capogrossi MC, Gaetano C. Nepsilon-lysine acetylation determines dissociation from GAP junctions and lateralization of connexin 43 in normal and dystrophic heart. *Proc Natl Acad Sci U S A* 2011;**108**:2795–2800.
15. Brandenburger M, Wenzel J, Bogdan R, Richardt D, Nguemo F, Reppel M, Hescheler J, Terlau H, Dendorfer A. Organotypic slice culture from human adult ventricular myocardium. *Cardiovasc Res.* 2012;**93**:50–59.
16. Piacentini R, Ripoli C, Leone L, Misiti F, Clementi ME, D'Ascenzo M, Giardina B, Azzena GB, Grassi C. Role of methionine 35 in the intracellular Ca2+ homeostasis dysregulation and Ca2+-dependent apoptosis induced by amyloid beta-peptide in human neuroblastoma IMR32 cells. *J Neurochem* 2008;**107**:1070–1082.
17. Piacentini R, Ripoli C, Mezzogori D, Azzena GB and Grassi C. Extremely low-frequency electromagnetic fields promote in vitro neurogenesis via upregulation of Ca(v)1-channel activity. *J Cell Physiol* 2008;**215**:129–139.
18. Rosati J, Spallotta F, Nanni S, Grasselli A, Antonini A, Vincenti S, Presutti C, Colussi C, D'Angelo C, Biroccio A, Farsetti A, Capogrossi MC, Illi B, Gaetano C. Smad-interacting protein-1 and microRNA 200 family define a nitric oxide-dependent molecular circuitry involved in embryonic stem cell mesendoderm differentiation. *Arterioscler Thromb Vasc Biol* 2011;**31**:898–907.
19. Nanni S, Benvenuti V, Grasselli A, Priolo C, Aiello A, Mattiussi S, Colussi C, Lirangi V, Illi B, D'Eletto M, Cianciulli AM, Gallucci M, De Carli P, Sentinelli S, Mottolese M, Carlini P, Strigari L, Finn S, Mueller E, Arcangeli G, Gaetano C, Capogrossi MC, Donnorso RP, Bacchetti S, Sacchi A, Pontecorvi A, Loda M, Farsetti A. Endothelial NOS, estrogen receptor beta, and HIFs cooperate in the activation of a prognostic transcriptional pattern in aggressive human prostate cancer. *J Clin Invest* 2009;**119**:1093–1108.
20. Spallotta F, Tardivo S, Nanni S, Rosati JD, Straino S, Mai A, Vecellio M, Valente S, Capogrossi MC, Farsetti A, Martone J, Bozzoni I, Pontecorvi A, Gaetano C, Colussi C. Detrimental effect of class-selective histone deacetylase inhibitors during tissue regeneration following hindlimb ischemia. *J Biol Chem* **288**:22915–22929.
21. D'Ascenzo M, Vairano M, Andreassi C, Navarra P, Azzena GB, Grassi C. Electrophysiological and molecular evidence of L-(Cav1), N- (Cav2.2), and R-(Cav2.3) type Ca2+ channels in rat cortical astrocytes. *Glia* 2004;**45**:354–363.
22. Brenman JE, Chao DS, Xia H, Aldape K, Bredt DS. Nitric oxide synthase complexed with dystrophin and absent from skeletal muscle sarcolemma in Duchenne muscular dystrophy. *Cell* 1995;**82**:743–752.
23. Capelson M, Liang Y, Schulte R, Mair W, Wagner U, Hetzer MW. Chromatin-bound nuclear pore components regulate gene expression in higher eukaryotes. *Cell* 2010;**140**:372–383.
24. Vaquerizas JM, Suyama R, Kind J, Miura K, Luscombe NM, Akhtar A. Nuclear pore proteins nup153 and megator define transcriptionally active regions in the Drosophila genome. *PLoS Genet* 2010;**6**:e1000846.
25. Finsterer J, Stollberger C. The heart in human dystrophinopathies. *Cardiology* 2003;**99**:1–19.
26. Choudhary C, Kumar C, Gnad F, Nielsen ML, Rehman M, Walther TC, Olsen JV, Mann M. Lysine acetylation targets protein complexes and co-regulates major cellular functions. *Science* 2009;**325**:834–840.
27. Kaypee S, Sudarshan D, Shanmugam MK, Mukherjee D, Sethi G, Kundu TK. Aberrant lysine acetylation in tumorigenesis: implications in the development of therapeutics. *Pharmacol Ther* 2016;**162**:98–119.
28. Swaminathan G, Rossi F, Sierra LJ, Gupta A, Navas-Martin S, Martin-Garcia J. A role for microRNA-155 modulation in the anti-HIV-1 effects of Toll-like receptor 3 stimulation in macrophages. *PLoS Pathog* 2012;**8**:1–23.
29. Chow KH, Elgort S, Dasso M, Ullman KS. Two distinct sites in Nup153 mediate interaction with the SUMO proteases SENP1 and SENP2. *Nucleus* 2012;**3**:349–358.
30. Kodiha M, Tran D, Qian C, Morogan A, Presley JF, Brown CM, Stochaj U. Oxidative stress mislocalizes and retains transport factor importin-alpha and nucleoporins Nup153 and Nup88 in nuclei where they generate high molecular mass complexes. *Biochim Biophys Acta* 2008;**1783**:405–418.
31. Luthra R, Kerr SC, Harreman MT, Apponi LH, Fasken MB, Ramineni S, Chaurasia S, Valentini SR, Corbett AH. Actively transcribed GAL genes can be physically linked to the nuclear pore by the SAGA chromatin modifying complex. *J Biol Chem* 2007;**282**:3042–3049.
32. Gabrielsen A, Lawler PR, Yongzhong W, Steinbruchel D, Blagoja D, Paulsson-Berne G, Kastrup J, Hansson GK. Gene expression signals involved in ischemic injury, extracellular matrix composition and fibrosis defined by global mRNA profiling of the human left ventricular myocardium. *J Mol Cell Cardiol* 2007;**42**:870–883.
33. Maltsev AV, Kokoz YM, Evdokimovskii EV, Pimenov OY, Reyes S, Alekseev AE. Alpha-2 adrenoceptors and imidazoline receptors in cardiomyocytes mediate counterbalancing effect of agmatine on NO synthesis and intracellular calcium handling. *J Mol Cell Cardiol* 2014;**68**:66–74.
34. Mayr B, Montminy M. Transcriptional regulation by the phosphorylation-dependent factor CREB. *Nat Rev Mol Cell Biol* 2001;**2**:599–609.
35. Kirchhof P, Marijon E, Fabritz L, Li N, Wang W, Wang T, Schulte K, Hanstein J, Schulte JS, Vogel M, Mougenot N, Laakmann S, Fortmueller L, Eckstein J, Verheule S, Kaese S, Staab A, Grote-Wessels S, Schotten U, Moubarak G, Wehrens XH, Schmitz W, Hatem S, Muller FU. Overexpression of cAMP-response element modulator causes abnormal growth and development of the atrial myocardium resulting in a substrate for sustained atrial fibrillation in mice. *Int J Cardiol* 2013;**166**:366–374.
36. Hassel D, Dahme T, Erdmann J, Meder B, Huge A, Stoll M, Just S, Hess A, Ehlermann P, Weichenhan D, Grimmler M, Liptau H, Hetzer R, Regitz-Zagrosek V, Fischer C,

Nurnberg P, Schunkert H, Katus HA, Rottbauer W. Nexilin mutations destabilize cardiac Z-disks and lead to dilated cardiomyopathy. *Nat Med* 2009;**15**:1281–1288.
37. Wang H, Li Z, Wang J, Sun K, Cui Q, Song L, Zou Y, Wang X, Liu X, Hui R, Fan Y. Mutations in NEXN, a Z-disc gene, are associated with hypertrophic cardiomyopathy. *Am J Hum Genet* 2010;**87**:687–693.
38. Pignier C, Ancey C, Fares N, Bescond J, Potreau D. Reexpression of the nifedipine-resistant calcium channel during dedifferentiation of adult rat ventricular cardiomyocytes. *J Cardiovasc Electrophysiol* 2002;**13**:178–183.
39. Koenig X, Rubi L, Obermair GJ, Cervenka R, Dang XB, Lukacs P, Kummer S, Bittner RE, Kubista H, Todt H, Hilber K. Enhanced currents through L-type calcium channels in cardiomyocytes disturb the electrophysiology of the dystrophic heart. *Am J Physiol Heart Circ Physiol* 2014;**306**:H564–H573.
40. Muntoni F, Torelli S, Ferlini A. Dystrophin and mutations: one gene, several proteins, multiple phenotypes. *Lancet Neurol* 2003;**2**:731–740.
41. Ahn AH, Kunkel LM. The structural and functional diversity of dystrophin. *Nat Genet* 1993;**3**:283–291.